International Journal of Heat and Mass Transfer 54 (2011) 3732–3739

Contents lists available at ScienceDirect

International Journal of Heat and Mass Transfer

journal homepage: www.elsevier.com/locate/ijhmt

Cooling augmentation using microchannels with rotatable separating plates

A.-R.A. Khaled [a], K. Vafai [b,*]

[a] Department of Thermal Engineering and Desalination Technology, King Abdulaziz University, P.O. Box 80204, Jeddah 21589, Saudi Arabia
[b] Department of Mechanical Engineering, University of California, Riverside, Riverside, CA 92521, USA

ARTICLE INFO

Article history:
Received 9 January 2011
Received in revised form 9 February 2011
Accepted 9 February 2011
Available online 21 April 2011

Keywords:
Flexible
Microheat exchanger
Microchannel
Convection
Seals

ABSTRACT

Cooling augmentation using double layered (DL) microchannels separated by rotatable plates is investigated in this work. The analyzed devices of the proposed configuration are (A) the flexible microheat exchanger, and (B) the DL-flexible microchannel device. The moment of the pressure forces on the separating plate is related to its rotational angle through its flexible supports. Energy equations for the flowing fluids are solved numerically using an iterative finite-difference method. Comparisons with obtained closed-form solutions under fully developed conditions are performed and excellent agreement is obtained. It is found that the effectiveness and the heat transfer rate per unit pumping power for the flexible microheat exchanger are always higher than that for the rigid one. Moreover, DL-flexible microchannels devices are found to provide more cooling effects per unit pumping power than rigid ones at flow Reynolds numbers below specific values, and at stiffness number and aspect ratio above certain values. These specific values are found to vary with the magnitude of the heating load. DL-microchannels with rotatable separating plates can be utilized in several applications such as electronic cooling.

1. Introduction

Many electronic devices incorporate large integration density of chips in a small area such as VLSI components. These devices consume large amount of electrical energy which is dissipated as heat. The amount of dissipated heat is usually very large and can be more than 100 W/cm^2 [1]. As such, conventional cooling technologies may not work. Recent developments in microfabrication technologies have enabled readily accessible fabrication of microchannel heat sinks primarily for cooling of electronic components [2–8]. These devices can be arranged in a single layered (SL) micro-passages such as those described in the works of Lee and Vafai [9] and Fedorov and Viskanta [10]. In addition, they can be arranged in double layered (DL) microchannel passages which was invented and reported by Vafai and Zhu [11]. DL-microchannels are found to provide additional cooling capacity and they can decrease the coolant temperature gradients along the microchannel length. It should be mentioned that SL-microchannel heat sinks can be either single microchannel system [12] or multiple microchannel system [9]. Microchannels can have a wavy shape [13] in order to enhance heat transfer. The successive developments in microchannels technologies have revealed certain designs that are capable to increase fluid mixing within the fluid volume hence increasing the heat transfer passively [14].

The main disadvantage of conventional microchannel cooling devices is the increased coolant temperature as very large heating loads are dissipated by a relatively small coolant flow rates. As such, Vafai and Zhu [9] proposed the DL-microchannels heat sink devices. Another solution is to utilize flexible microchannels. These types of microchannels which were developed in the works of Khaled and Vafai [15–17] and Vafai and Khaled [18] reduce the coolant temperature because volumes of both the flow passage and the supporting seals are expandable. This effect causes an increase in the coolant flow rate. The volume expansion in flexible microchannels is due to pressure forces. These forces can be due to an increase in the pressure drop across the microchannel [18]. Also, it can be due to gas pressure if the supporting seals contain closed gas-cavities in contact with the heated surface. As such, any increase in the gas pressure due to excessive heating produces extra expansion in the volume [15,17]. As the expansion in the flow passage volume may result in slight reduction in the convection heat transfer coefficient [18], a new configuration of DL-flexible microchannels device is considered here.

In this work, a DL-microchannel cooling device with rotatable separating plate is proposed and analyzed for possible augmenting in the cooling effects. The separating plate is assumed to be supported via anti-leaking flexible seals. The only allowable motion for that plate is the rotational motion about a pivot rod. This rod is taken to be aligned along the microchannel center line normal to its sides boundaries. Two different devices based on the above configuration are considered. They are (A) the flexible micro heat exchanger and (B) the heated DL-flexible microchannel device.

* Corresponding author. Tel.: +1 951 827 2135; fax: +1 951 827 2899.
E-mail address: vafai@engr.ucr.edu (K. Vafai).

0017-9310/$ - see front matter © 2011 Elsevier Ltd. All rights reserved.
doi:10.1016/j.ijheatmasstransfer.2011.02.054

Nomenclature

A_d	maximum relative displacement of the separating plate, d/H_o
A_k	cold to hot fluids thermal conductivities ratio, k_c/k_h
$A\mu$	cold to hot fluids dynamic viscosities ratio, μ_c/μ_h
$A\rho$	cold to hot fluids densities ratio, ρ_c/ρ_h
C_c, C_h	cold and hot fluids thermal capacities per unit width [W m^{-1} K^{-1}]
d	maximum displacement of the separating plate [m]
E_o	dimensionless elastic parameter defined in Eq. (11)
H	microchannel height [m]
$\bar{H}$	microchannel dimensionless height defined in Eq. (1)
H_o	half main microchannel height [m]
h	convection heat transfer coefficient [W m^{-2} K^{-1}]
K	stiffness of the supporting seals per unit separating plate width [N]
Ka	stiffness number defined in Eq. (30)
k	thermal conductivity [W m^{-2} K^{-1}]
L	microchannel length [m]
Nu	local Nusselt number defined Eqs. (47), (48) and (62)
P_t	total ideal pumping power requirement [W m^{-1}]
p	mean pressure [N m^{-2}]
q'	heat transfer rate per unit width [W m^{-1}]
Pr	Prandtl number, $\mu c_p/k$
Re	Reynolds number, $\rho u_h H_o/\mu$
T	temperature field [K]
T_m	mean bulk temperature [K]
U	local overall heat transfer coefficient [W m^{-2} K^{-1}]
U_e	equivalent overall heat transfer coefficient [W m^{-2} K^{-1}]
u	velocity field [m s^{-1}]
$\bar{u}$	dimensionless velocity field defined in Eqs. (19) and (20)
x	axial micro-passage coordinate [m]
$\bar{x}$	dimensionless axial micro-passage coordinate defined in Eqs. 3(c, d)
y	transverse micro-passage coordinate [m]
$\bar{y}$	dimensionless transverse coordinates defined in Eqs. 18(a, b)

Greek symbols

ε	effectiveness of the heat exchanger defined in Eq. (43)
ε_c, ε_h	effectiveness of cold and hot fluids flows defined in Eqs. (35) and (36)
$\gamma_1\gamma_2$	first and second performance indicators defined in Eqs. (44) and (64)
λ_s	dimensionless maximum heated plate temperature defined in Eq. (63)
μ	fluid dynamic viscosity [kg m^{-1} s^{-1}]
θ	dimensionless temperature defined in Eqs. 18(c, d)
θ_m	mean bulk dimensionless temperature defined in Eqs. (41) and(42)
P	dimensionless ideal pumping power requirement defined in Eq. (33)
ρ	fluid density [kg m^{-3}]

Subscripts

1	inlet
2	exit
c	cold fluid
fd	thermally fully developed
h	hot fluid
m	mean value

The linear elasticity theory [19] is applied to flexible seals supporting the separating plate to relate the moment of the pressure forces on that plate to its rotational angle. The energy equations for both fluids are solved numerically for general conditions and analytically under special conditions. As such, the effectiveness of the flexible micro heat exchanger (device A) and other performance indicators for both devices (A) and (B) are calculated. The advantages of the proposed device in cooling attributes over the performance of the DL-rigid microchannel device are examined.

2. Problem formulation

2.1. Modeling of the maximum relative displacement of the moving plate

Consider a wide microchannel of height $2H_o$ which is much smaller than its length L. Consider that this microchannel is divided into two identical microchannels by a highly conductive and inflexible separating plate mounted about a pivot axis (O). The pivot axis is taken to be a rod aligned along the normal centerline axis of the device as seen in (Fig. 1). Accordingly, the allowable motion of the separating plate is the rotational motion about that pivot axis. Two fluids at different temperatures are allowed to flow in counter-direction inside the lower and upper microchannels. The hot fluid which is at temperature T_{h1} enters the lower microchannel and flows towards the left direction along the x_h-axis as shown in Fig. 1. However, the cold fluid which is at temperature $T_{c1}(T_{c1} < T_{h1})$ is allowed to flow in the upper microchannel towards right direction along and the x_c-axis as shown in Fig. 1. The heights

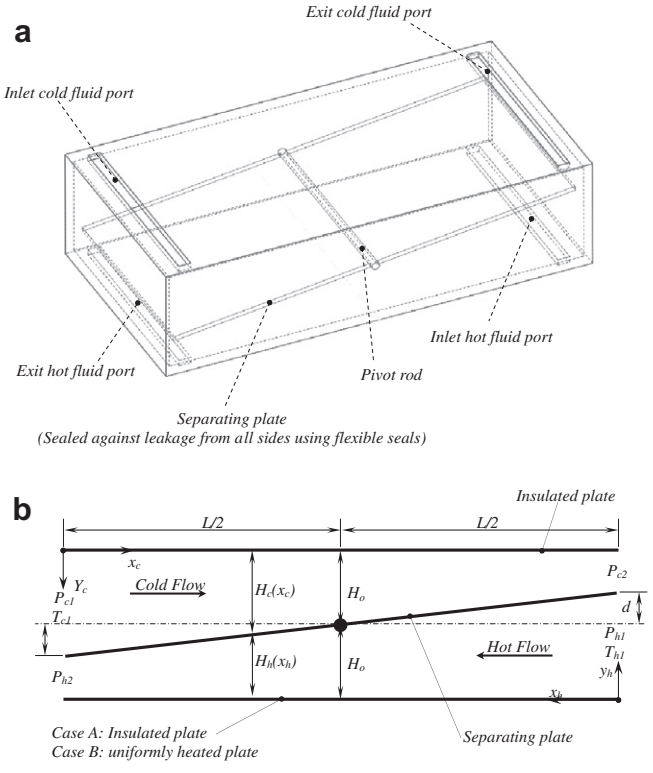

Fig. 1. (a) 3D view of the DL-microchannel device with rotatable separating plate, and (b) side view schematic of the device and the coordinate system.

of the microchannels denoted by $H_{h,c}(H_h$ and $H_c)$ vary with the axial coordinates according to the following relationships [20]:

$$\overline{H}_{h,c}(\bar{x}_{h,c}) \equiv \frac{H_{h,c}(\bar{x}_{h,c})}{H_o} = 1 + A_d\{1 - 2A_r\bar{x}_{h,c}\}. \quad (1,2)$$

The subscript "h" stands for the hot fluid while the subscript "c" stands for the cold fluid. The parameters A_d, A_r and the dimensionless variable $\bar{x}$ are the maximum relative displacement of separating plate, the aspect ratio and the dimensionless axial coordinate, respectively. They are given by

$$A_d = \frac{d}{H_o}; \quad A_r = \frac{H_o}{L}; \quad \bar{x}_{h,c} = \frac{x_{h,c}}{L}, \quad (3a\text{-}d)$$

where d is the maximum displacement of the separating plate

The width of the microchannel is taken to be much larger than its height in order to have enough pressure forces to cause rotation of the separating plate. As such, the two-dimensional flow model [18] is adopted here and the steady state Reynolds equations for the microchannels are given by

$$\frac{d}{dx_{h,c}}\left(H_{h,c}^3\frac{dp_{h,c}}{dx_{h,c}}\right) = 0, \quad (4,5)$$

where p_h and p_c are the mean pressures inside the lower and upper microchannels, respectively. The solution to Eqs. (4) and (5) can be arranged in the following form:

$$\frac{p_{h,c}(\bar{x}_{h,c}) - p_{h1,c1}}{p_{h2,c2} - p_{h1,c1}} = \frac{1 - \left(\frac{1+A_d}{\overline{H}(\bar{x}_{h,c})}\right)^2}{1 - \left(\frac{1+A_d}{1-A_d}\right)^2}, \quad (6,7)$$

where p_{h1} and p_{h2} are the inlet and exit pressures of the hot fluid, respectively. Moreover, p_{c1} and p_{c2} are the inlet and exit pressures of the cold fluid, respectively.

We allow the motion of the separating plate to be restrained by the stiffness effect of the elastic seals supporting it [18]. As such, the net moment of pressure forces applied on that plate about the pivot axis per unit width, $\sum M'_o$, is equal to

$$\sum M'_0 = K\tan^{-1}(2d/L), \quad (8)$$

where K is the stiffness of the supporting seals per unit width of the separating plate. When $A_r < 0.05$ as in microchannel applications, the rotational angle which is equal to $\tan^{-1}(2d/L)$ can be approximated by the value $(2d/L)$. Also it should be noted that $\sum M'_o$ is equal to the following expression when $A_r < 0.05$:

$$\sum M'_0 = \int_0^L p_h\{L/2 - x_h\}dx_h - \int_0^L p_c\{x_c - L/2\}dx_c. \quad (9)$$

Substituting Eq. (9) into Eq. (8) while utilizing Eqs. (6) and (7) and solving Eq. (8) yields the following relationship:

$$\frac{\left\{1 - \left(\frac{1+A_d}{1-A_d}\right)^2\right\}\left\{\frac{A_d^2}{1+A_d}\right\}}{\left(\frac{1+A_d}{2A_d}\right)\ln\left(\frac{1+A_d}{1-A_d}\right) - \left(\frac{1}{1-A_d}\right)} = E_o, \quad (10)$$

where E_o is the dimensionless elastic parameter which is equal to

$$E_o = \frac{(p_{h1} - p_{h2}) + (p_{c1} - p_{c2})}{4KA_r/L^2}. \quad (11)$$

It is difficult to obtain the inverse of Eq. (11) analytically. However utilizing statistical softwares, A_d is correlated to E_o by the following functional form:

$$A_d = \frac{a_1 + a_2E_o + a_3E_o^2 + a_4E_o^3 + a_5E_o^4}{1 + a_6E_o^4 + a_7E_o^4 + a_8E_o^4 + a_9E_o^4}. \quad (12)$$

The following a_1–a_9 coefficients were found to produce the correlation coefficient $R^2 = 1.0$ for 999 equally spaced A_d-values (maximum deviation of A_d from exact is 1.48% at $A_d = 0.001$):

$$a_1 = -1.59176\times10^{-5}; \quad a_2 = 0.166851; \quad a_3 = 0.0661679;$$
$$a_4 = 0.0161819; \quad a_5 = 0.00150295; \quad a_6 = 0.399939;$$
$$a_7 = 0.116314; \quad a_8 = 0.0192561; \quad a_9 = 0.00150283; \quad (13a\text{-}i)$$

2.2. Modeling of flow and heat transfer inside the two microchannels

Both fluids are considered to be Newtonian fluids having constant average properties though compressible fluids can be used in microchannel applications [21]. The momentum and energy equations inside each microchannel are given by [18]:

$$0 = -\frac{dp_{h,c}}{dx_{h,c}} + \mu_{h,c}\frac{\partial^2 u_{h,c}}{\partial y_{h,c}^2}, \quad (14,15)$$

$$\rho_{h,c}(c_p)_{h,c}u_{h,c}\frac{\partial T_{h,c}}{\partial x_{h,c}} = k_{h,c}\frac{\partial^2 T_{h,c}}{\partial y_{h,c}^2}, \quad (16,17)$$

where μ, u, T, ρ, c_p and k are the dynamic viscosity of the fluid, velocity field, temperature field, fluid density, fluid specific heat and the fluid thermal conductivity, respectively. Define the following dimensionless variables:

$$\bar{y}_{h,c} = \frac{y_{h,c}}{H(x_{h,c})}; \quad \theta_{h,c} = \frac{T_{h,c}(\bar{x}_{h,c},\bar{y}_{h,c}) - T_{h1,c1}}{T_{c1,h1} - T_{h1,c1}}. \quad (18a\text{-}d)$$

The dimensionless velocity fields $\bar{u}_{h,c}(\bar{y}_{h,c})$ are obtained by solving Eqs. (14) and (15). This will result

$$\bar{u}_{h,c}(\bar{y}_{h,c}) = \frac{u_{h,c}(\bar{x}_{h,c},\bar{y}_{h,c})}{u_{hm,cm}(\bar{x}_{h,c})} = 6\bar{y}_{h,c}(1 - \bar{y}_{h,c}) \quad (19,20)$$

The mean velocities $u_{hm}(\bar{x}_h)$ and $u_{cm}(\bar{x}_c)$ are related to pressure gradients inside the microchannels according to the following relationships:

$$u_{hm,cm}(\bar{x}_{h,c}) = \frac{-H_o^2}{12\mu_{h,c}}\frac{dp_{h,c}}{dx_{h,c}}\left[\overline{H}_{h,c}(\bar{x}_{h,c})\right]^2 = \frac{u_{hmo,cmo}}{\overline{H}_{h,c}(\bar{x}_{h,c})}CF, \quad (21,22)$$

where u_{hmo} and u_{cmo} are the mean velocities of the hot and cold fluids when $d = 0$, respectively. The quantities u_{hmo} and u_{cmo} and the mean velocities correction factor CF are given by

$$u_{hmo,cmo} = \frac{1}{12\mu_{h,c}}\left(\frac{\Delta p_{h,c}}{L}\right)H_o^2, \quad (23,24)$$

$$CF = \frac{4A_d(1+A_d)^2}{\left(\frac{1+A_d}{1-A_d}\right)^2 - 1}, \quad (25)$$

where $\Delta p_h = p_{h1} - p_{h2}$ and $\Delta p_c = p_{c1} - p_{c2}$.

Imposing the variables given in Eqs. (3) and (18), on Eqs. (16) and (17) results in the following dimensionless equations:

$$Re_{h,c}\,Pr_{h,c}(CF)\bar{u}_{h,c}\overline{H}_{h,c}\frac{\partial\theta_{h,c}}{\partial\bar{x}_{h,c}} = \frac{\partial^2\theta_{h,c}}{\partial\bar{y}_{h,c}^2}, \quad (26,27)$$

where Re and Pr are the Reynolds number and the Prandtl number, respectively. The Reynolds numbers are defined based on the following expressions:

$$Re_{h,c} = \frac{\rho_{h,c}u_{hmo,cmo}H_o}{\mu_{h,c}} \quad (28a,b)$$

The dimensionless parameter E_o can be expressed in terms of the flow Reynolds numbers as follows:

$$E_o = \frac{3}{A_r^4 Ka}\left\{\left(\frac{A_\rho}{A_\mu^2}\right)Re_h + Re_c\right\}, \tag{29}$$

where Ka, $A\rho$ and $A\mu$ which are given below are the dimensionless stiffness number, cold to hot fluid density ratio and cold to hot fluid dynamic viscosity ratio, respectively:

$$Ka = \frac{K}{\mu_c^2/\rho_c}; \quad A_\rho = \frac{\rho_c}{\rho_k}; \quad A_\mu = \frac{\mu_c}{\mu_k}. \tag{30-32}$$

2.3. The ideal total pumping power requirement

The total ideal pumping power requirements, P_t, can be expressed in terms of the dimensionless parameters as follows:

$$P \equiv \frac{P_t}{\mu_c^3/(\rho_c^2 H_o^2)} = \frac{\Delta p_h \dot{m}_h/\rho_h + \Delta p_c \dot{m}_c/\rho_c}{\mu_c^3/(\rho_c^2 H_o^2)} = \frac{12}{A_r}\left\{Re_c^2 + \left(\frac{A_\rho^2}{A_\mu^3}\right)Re_h^2\right\}CF, \tag{33}$$

where $\dot{m}_h$ and $\dot{m}_c$ are the mass flow rate of hot and cold fluids, respectively.

2.3.1. Case (A): insulated DL-microchannels with rotatable separating plate (flexible micro heat exchanger case)

The boundary conditions for this case are given by

$$\theta_h(\bar{x}_h = 0, \bar{y}_h) = 0; \quad \theta_c(\bar{x}_c = 0, \bar{y}_c) = 0 \tag{34a, b}$$

$$\theta_c(\bar{x}_c = 1/A_r - \bar{x}_h, \bar{y}_c = 1) = 1 - \theta_h(\bar{x}_h, \bar{y}_c = 1), \tag{34c}$$

$$\left.\frac{\partial\theta_h}{\partial\bar{y}_h}\right|_{\bar{x}_h,\bar{y}_h=1.0} = A_k\left\{\frac{\overline{H}_h(\bar{x}_h)}{H_c(\bar{x}_c = 1/A_r - \bar{x}_h)}\right\}\left.\frac{\partial\theta_c}{\partial\bar{y}_c}\right|_{\bar{x}_c=1/A_r-\bar{x}_h,\bar{y}_c=1.0}, \tag{34d}$$

$$\left.\frac{\partial\theta_h}{\partial\bar{y}_h}\right|_{\bar{x}_h,\bar{y}_h=0} = \left.\frac{\partial\theta_c}{\partial\bar{y}_c}\right|_{\bar{x}_c,\bar{y}_c=0} = 0, \tag{34e, f}$$

where $A_k = k_c/k_h$. For this case, the effectivenesses of the hot and cold fluids, ε_h and ε_c are defined as follows:

$$\varepsilon_{h,c} \equiv \frac{q'}{\dot{m}_{h,c}(c_p)_{h,c}(T_{h1} - T_{c1})} = \frac{q'}{(\rho c_p)_{h,c} u_{hm,cm} H_{h,c}(T_{h1} - T_{c1})}, \tag{35, 36}$$

where q' is the rate of heat transfer between the two fluids per unit width. Recall that q' is given by

$$q' = (\rho c_p)_h u_{hm} H_h\{T_{h1} - T_{hm2}\} = (\rho c_p)_c u_{cm} H_c\{T_{cm2} - T_{c1}\}, \tag{37, 38}$$

where T_{hm2} and T_{cm2} are the mean bulk temperature at the exit of the hot and cold fluids, respectively. The mean bulk temperatures are given by:

$$T_{hm,cm} = \int_0^{H_{h,c}}\left\{\frac{u_{h,c}}{u_{hm,cm}}\right\}T_{h,c}\,dy_{h,c}. \tag{39, 40}$$

In terms of the dimensionless parameters, the parameters ε_h and ε_c are given by

$$\varepsilon_{h,c} = \theta_{hm,cm}(\bar{x}_{h,c} = 1/A_r) = \int_0^1 \bar{u}_{h,c}(\bar{y}_{h,c})\theta_h(\bar{x}_{h,c} = 1/A_r, \bar{y}_{h,c})\,d\bar{y}_{h,c}. \tag{41, 42}$$

Accordingly, the effectiveness of the micro heat exchanger, ε, which is the maximum value of ε_h and ε_c [22] can be expressed by

$$\varepsilon = \begin{cases} \varepsilon_h & \text{if} \quad \varepsilon_h > \varepsilon_c \\ \varepsilon_c & \text{if} \quad \varepsilon_c > \varepsilon_h \end{cases} \tag{43}$$

Lets define the first performance indicator, γ_1, as the ratio of the rate of heat transfer between the two fluids per its ideal total pumping power requirement to that of the rigid micro heat exchanger (case with $E_o = 0$). This can be expressed by

$$\gamma_1 = \left\{\frac{\varepsilon}{\varepsilon_{E_o=0}}\right\}CF\left(\frac{P_t|_{E_o}=0}{P_t}\right) = \frac{\varepsilon}{\varepsilon_{E_o=0}}. \tag{44}$$

The local hot and cold flows convection heat transfer coefficients h_h and h_c, respectively, are defined as

$$h_{h,c}\{T_{hm,cm}(x_{h,c}) - T_{h,c}(x_{h,c}, y_{h,c} = H_{h,c})\} = -k_{h,c}\left.\frac{\partial T_{h,c}}{\partial y_{h,c}}\right|_{x_{h,c},y_{h,c}=H_{h,c}}. \tag{45, 46}$$

Thus, the local hot and cold section Nusselt numbers Nu_h and Nu_c are equal to

$$Nu_{h,c} \equiv \frac{h_{h,c}H_{h,c}}{k_{h,c}} = \frac{1}{\{\theta_{hm,cm}(\bar{x}_{h,c}) - \theta_h(\bar{x}_{h,c}, \bar{y}_{h,c} = 1)\}}\left(-\left.\frac{\partial\theta_{h,c}}{\partial\bar{y}_{h,c}}\right|_{\bar{x}_{h,c},\bar{y}_{h,c}=1}\right) \tag{47, 48}$$

2.3.1.1. Approximate analytical solution for fully developed conditions. Under fully developed conditions, axial gradient of the temperature difference across any section of the flexible micro heat exchanger can be considered to be very small. Accordingly, $Nu_h \cong Nu_c \cong Nu_{fd} = 2.695$ [23]. The latter number is for the case of laminar flow between an insulated plate and a plate subject to a constant heat flux. The heat transfer rate across a differential element within the flexible micro heat exchanger containing both fluids is given by:

$$\begin{aligned}\delta q' &= -C_h dT_{hm} = -C_c dT_{cm} = U\{T_{hm} - T_{cm}\}dx_h \\ &= \left\{\frac{T_{hm} - T_{cm}}{(1/h_h) + (1/h_c)}\right\}dx_h,\end{aligned} \tag{49a-d}$$

where $C_h = \rho_h(c_p)_h u_{hm} H_h$ and $C_c = \rho_c(c_p)_c u_{cm} H_c$. Note that U is the overall heat transfer coefficient. In terms of dimensionless parameters, Eq. 49(c) can be expressed as

$$\delta q' = \left\{\frac{Nu_{fd}}{\overline{H}_h\{A_k - 1\} + 2}\right\}\left(\frac{T_{hm} - T_{cm}}{H_o/k_c}\right)dx_h. \tag{50}$$

The differential of the mean bulk temperatures difference across any section can be obtained using Eqs. 49(a–c) as

$$\frac{d(T_{hm} - dT_{cm})}{T_{hm} - T_{cm}} = -\left(\frac{1}{C_h} - \frac{1}{C_c}\right)\left\{\frac{Nu_{fd}k_c/H_o}{\overline{H}_h\{A_k - 1\} + 2}\right\}dx_h. \tag{51}$$

Integrating both sides of Eq. (51) over the micro heat exchanger length results in the following expression:

$$\frac{T_{hm2} - T_{c1}}{T_{h1} - T_{cm2}} = \left(\frac{A_k + \left\{\frac{1+A_d}{1-A_d}\right\}}{1 + A_k\left\{\frac{1+A_d}{1-A_d}\right\}}\right)^{\Phi}. \tag{52}$$

The power Φ is given by

$$\Phi = \left(\frac{A_k}{Pe_h} - \frac{1}{Pe_c}\right)\left\{\frac{Nu_{fd}}{2A_rA_d(A_k - 1)CF}\right\}. \tag{53}$$

Using Eqs. (35) and (52) ε_h can be represented as

$$\varepsilon_h = \frac{1 - \left\{\left(A_k + \left\{\frac{1+A_d}{1-A_d}\right\}\right)\Big/\left(1 + A_k\left\{\frac{1+A_d}{1-A_d}\right\}\right)\right\}^{\Phi}}{1 - \left(\frac{Pe_h}{A_kPe_c}\right)\left\{\left(A_k + \left\{\frac{1+A_d}{1-A_d}\right\}\right)\Big/\left(1 + A_k\left\{\frac{1+A_d}{1-A_d}\right\}\right)\right\}^{\Phi}}. \tag{54}$$

Similarly, using Eqs. (36) and (52), ε_c can be represented as

$$\varepsilon_c = \frac{1 - \left\{\left(A_k + \left\{\frac{1+A_d}{1-A_d}\right\}\right)\Big/\left(1 + A_k\left\{\frac{1+A_d}{1-A_d}\right\}\right)\right\}^{\Phi}}{\left(\frac{A_kPe_c}{Pe_h}\right) - \left\{\left(A_k + \left\{\frac{1+A_d}{1-A_d}\right\}\right)\Big/\left(1 + A_k\left\{\frac{1+A_d}{1-A_d}\right\}\right)\right\}^{\Phi}}. \tag{55}$$

Lets introduce $\varepsilon = MAX(\varepsilon_h, \varepsilon_c)$, as the nominal definition of the counter flow micro heat exchanger effectiveness [22], given by

$$\varepsilon = \frac{1-\exp(-NTU[1-C^*])}{1-C^*\exp(-NTU[1-C^*])}. \tag{56}$$

Accordingly, NTU will be the equivalent number of transfer units which is given by

$$NTU = \frac{U_e L}{(\rho c_p u_{mo})_{\min} H_o CF}, \tag{57}$$

where U_e is the equivalent overall heat transfer coefficient. Note that $C^* = C_{\min}/C_{\max}$ where C_{min} and C_{max} are the minimum and maximum values of C_h and C_c values, respectively. Utilizing Eqs. (54) and (55), the following relationship can be obtained:

$$\frac{U_e}{(U_e)_{Ka\to\infty}} = \left\{\frac{1}{2A_d(CF)}\right\}\left(\frac{1+A_k}{1-A_k}\right)\ln\left(\frac{A_k+(1+A_d)/(1-A_d)}{1+A_k(1+A_d)/(1-A_d)}\right). \tag{58}$$

2.3.2. Case (B): DL-microchannels with rotatable separating plates subject to uniform heat flux, q''_s, from below

The boundary condition given by Eq. 34(e) is changed for this case to the following:

$$\left.\frac{\partial\theta_h}{\partial\bar{y}_h}\right|_{\bar{x}_h,\bar{y}_h=0} = A_{q''}\overline{H}_h(\bar{x}_h), \tag{59}$$

where $A_{q''}$ is the dimensionless heat flux parameter which can be presented as

$$A_{q''} = \frac{q''_s H_o}{k_h(T_{h1}-T_{c1})}. \tag{60}$$

The local convection heat transfer coefficient for the heated plate side, h_s, is defined as

$$h_s\{T_h(x_h, y_h=0) - T_{hm}(x_h)\} = q''_s. \tag{61}$$

Thus, the local Nusselt number for the heated plate side, Nu_s, can be presented as

$$Nu_s \equiv \frac{h_s\overline{H}_h(\bar{x}_h)}{k_h} = \frac{-A_{q''}\overline{H}_h(\bar{x}_h)}{\{\theta_h(\bar{x}_h,\bar{y}_h=0)-\theta_{hm}(\bar{x}_h)\}}. \tag{62}$$

An important indicator for this case is the ratio of the difference between the maximum heated surface temperature and inlet cold fluid temperature to the difference between the hot and cold inlet temperatures. This ratio, which is represented by λ_s, is

$$\lambda_s \equiv \frac{[T_h(x_h,y_h=0)]_{\max}-T_{c1}}{T_{h1}-T_{c1}} = 1-[\theta_h(\bar{x}_h,\bar{y}_h=0)]_{\min}. \tag{63}$$

Defining the second performance indicator, γ_2, as the ratio of λ_s-value for the present heated DL-flexible micorchannel to that for the conventional rigid one (case with $Ka\to\infty$) when both operated under the same ideal pumping power, it can be presented by

$$\gamma_2 \equiv \left.\left(\frac{\lambda_s}{\lambda_s|_{K\to\infty}}\right)\right|_{P_t}. \tag{64}$$

The relation between the hot fluid Reynolds number for the present case, Re_h, and that for the conventional rigid one, Re_{hr}, that satisfies the constraint of Eq. (64) is given by

$$Re_h = \sqrt{\left(\frac{1}{CF}-1\right)\left(\frac{A_\mu^3}{A_\rho^2}\right)Re_c^2 + \frac{Re_{hr}^2}{CF}}, \tag{65}$$

when both microchannels have the same cold flow Reynolds number. Equation (65) can be solved by an iteration procedure, as CF is a function of both Re_c and Re_h.

3. Numerical methodology

Eqs. (26) and (27) which are coupled through their boundary conditions given by Eqs. 34(c,d), are solved numerically using an iterative method. The implicit-finite-difference method given by Blottner [24] is utilized for the present problem. These equations were discretized using three-points central differencing quotients for the first and second derivative terms with respect to $\bar{y}_h$ and $\bar{y}_c$ directions and an attempt was made to create a stable implicit finite difference scheme [25]. For the first derivative with respect to $\bar{x}_h$ and $\bar{x}_c$ directions, two points backward differencing quotients was used. The finite difference equations for Eqs. (26) and (27) along with their boundary conditions for the flexible microheat exchanger case are given by

$$Re_{h,c}Pr_{h,c}CF(\overline{H}_{h,c})_i(\bar{u}_{h,c})_j\left\{\frac{(\theta_{h,c})_{i,j}-(\theta_{h,c})_{i-1,j}}{\Delta\bar{x}_{h,c}}\right\} = \frac{(\theta_{h,c})_{i,j-1}-2(\theta_{h,c})_{i,j}+(\theta_{h,c})_{i,j+1}}{\Delta\bar{y}^2_{h,c}}, \tag{66,67}$$

$$\begin{aligned}
&(\theta_h)_{i=1,j} = (\theta_c)_{ii=1,jj} = 0,\\
&(\theta_h)_{i,j=N} = 1-(\theta_c)_{ii=M-i+1,jj=N},\\
&(\theta_h)_{i,j=N} = A_k(\overline{H}_h)_i\left\{\frac{(\theta_c)_{ii=M-i+1,jj=N}-(\theta_c)_{ii=M-i+1,jj=N-1}}{(\overline{H}_c)_{ii=M-i+1}}\right\}+(\theta_h)_{i,j=N-1},\\
&(\theta_h)_{i,j=1} = (\theta_h)_{i,j=2};\quad (\theta_c)_{ii,jj=1} = (\theta_c)_{ii,jj=2},
\end{aligned} \tag{68a-f}$$

where (i, j) and (ii, jj) are the location of the discretized points in the numerical grids for the lower and upper microchannels, respectively, and $\Delta\bar{x}_h$ and $\Delta\bar{x}_c$ are the distances between the two consecutive i and ii vertical lines in the numerical grid, respectively, and $\Delta\bar{y}_h$ and $\Delta\bar{y}_c$ are the distances between the two consecutive j and jj horizontal lines in the numerical grid, respectively.

The resulting tri-diagonal systems of algebraic equations obtained from discretizing Eqs. (66) and (67) at a given i and ii-sections, respectively, were solved using the Thomas algorithm [24]. The solution was based on an initial estimate of the temperature at the separating plate, $(\theta_h)_{i,j=N}$. The same procedure was repeated for the consecutive i and ii values while the temperatures at the separating plate were corrected using Eq. 68(d). The numerical results were compared with the analytical solution given earlier. An excellent agreement was found between the numerical and analytical results.

In what follows, both hot and cold fluids are taken to be liquid water. The maximum cold flow Reynolds number was taken as $Re_c = 33$. This corresponds to a cold flow mean velocity of $u_{cm} = 0.11$ m/s when the average height of the microchannel is $H_o = 300$ μm. The maximum stiffness number was taken as $Ka = 120\times10^6$. This corresponds to supporting seals stiffness per unit separating plate width of $K = 0.12$ N.

4. Results and discussion

4.1. Effect of E_o on the maximum relative displacement and CF-correction factor

The variations of the maximum displacement of the separating plate (A_d) and the mean velocity correction factor (CF) with the dimensionless elastic parameter, E_o, are shown in Fig. 2. The elastic parameter increases as the stiffness of the separating plate decreases. This effect increases the separating plate rotation causing an increase in A_d. As can be seen, the CF-mean velocity correction factor decreases as E_o increases. This effect is clearly seen in Fig. 2.

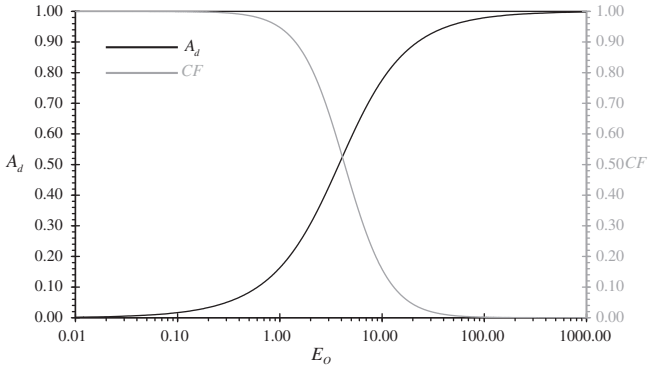

Fig. 2. Effects of the elastic parameter E_o on A_d and CF.

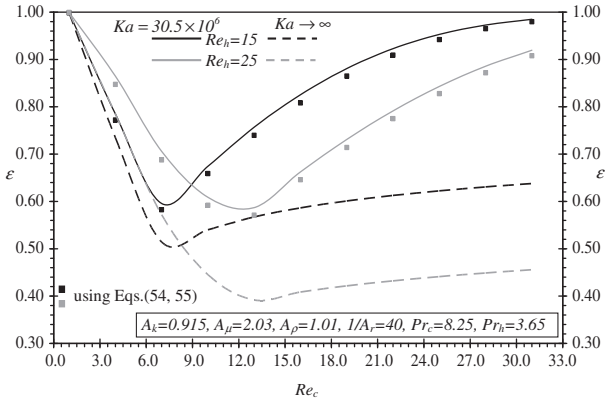

Fig. 4. Effects of Re_c on ε for the flexible micro heat exchanger case.

4.2. Flexible micro heat exchanger case

4.2.1. Nusselt number distributions and the validity of the analytical solution

Effects of the dimensionless axial distance ($\bar{x}$) and the aspect ratio (A_r) on the hot and cold fluid local Nusselt numbers (Nu_h, Nu_c), respectively, are illustrated in Fig. 3. This figure is presented for the case when both fluids have the same thermal capacitance ($Re_hPr_h = A_kRe_cPr_c$). For long microchannels such as when $1/A_r = 60$, both Nu_h and Nu_c converge to a constant value for most of $\bar{x}_h$-values. This value is very close to $Nu_{fd} = 2.695$. This corresponds to the case of fully developed channel flow between an insulated plate and a plate subject to constant heat flux. Thermal entry region effect is clearly seen in Fig. 3 for the case with $1/A_r = 10$, corresponding to short flexible micro heat exchangers. For this case, Both Nu_h and Nu_c decrease as distances from the inlet sections increase as shown in Fig. 3.

4.2.2. Variation of effectiveness and first performance indicator with Re_c

The variation of the flexible microheat exchanger effectiveness (ε) with the cold fluid Reynolds number (Re_c) is shown in Fig. 4. Also, shown in Fig. 4 is a comparison between analytical and numerical results. As it can be seen, there is an excellent agreement between these results. The increase in Re_c causes an increase in the cold fluid thermal capacitance (C_c). As Re_c approaches $Re_c = 7.256$ (when $Re_h = 15$) or $Re_c = 12.0881$ (when $Re_h = 25$), the value of C_c approaches C_h. This results in $\varepsilon_h = \varepsilon_c$ and produces the minimum effectiveness ($\varepsilon = \varepsilon_{min}$) as shown in Fig. 4. If $Re_c < 7.256$ (when $Re_h = 15$) or if $Re_c < 12.0881$ (when $Re_h = 25$), the temperature difference for the cold fluid is larger than that for the hot fluid thus, $\varepsilon = \varepsilon_c > \varepsilon_{min}$. However, $\varepsilon = \varepsilon_h > \varepsilon_{min}$ if $Re_c > 7.256$ (when $Re_h = 15$) or if $Re_c > 12.0881$ (when $Re_h = 25$). Therefore, ε decreases as Re_c increases until it reaches $\varepsilon = \varepsilon_{min}$ after which it starts to increase as Re_c increases as depicted in Fig. 5. For rigid micro heat exchangers ($K \to \infty$), the effectiveness is smaller than that for the flexible micro heat exchangers as shown in Fig. 4. It is noticed from Fig. 5 that the first performance indicator (γ_1) is always larger than one, indicating that the proposed flexible micro heat exchanger transfers more heat than the rigid one under constant pumping power. As such, the superiority of flexible micro heat exchangers over rigid ones is established.

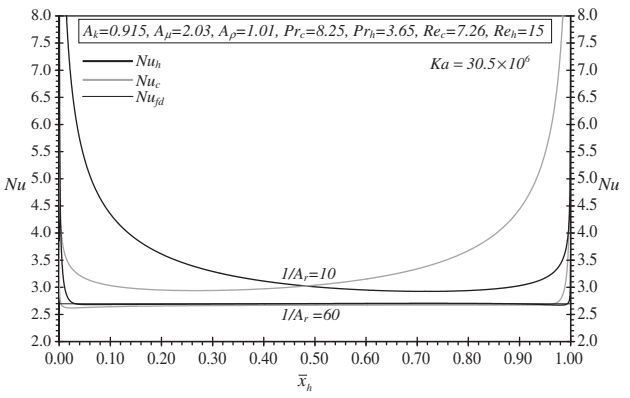

Fig. 3. Effects of $\bar{x}_h$ and A_r on Nu_h and Nu_c for the flexible micro heat exchanger case.

4.2.3. Variation of effectiveness and the first performance indicator with Ka

The increase in the dimensionless stiffness number (Ka) is accomplished by an increase in the supporting seals stiffness per unit width of the separating plate (K). As Ka decreases, the separating plate supporting seals softness increases. As such, the separating plate maximum relative displacement (A_d) increases as Ka decreases. As a consequence, velocities near the separating plate in regions very close to the fluids exits increases. Also, expansions of the microchannels near the inlet regions increase, which allow the thermal boundary layers to develop further downstream. Thus, convection heat transfer coefficients are expected to increase as Ka decreases. As such, ε increases as Ka decreases as can be seen in Fig. 6. Similarly, it is noticed from this figure that γ_1 is always larger than one and it increases as Ka decreases. Again, this estabilishes the superiority of flexible micro heat exchangers over rigid ones.

4.2.4. Variation of the first performance indicator with aspect ratio

The increase in the microchannel length causes a decrease in the aspect ratio. As such, the moment of the pressure forces across

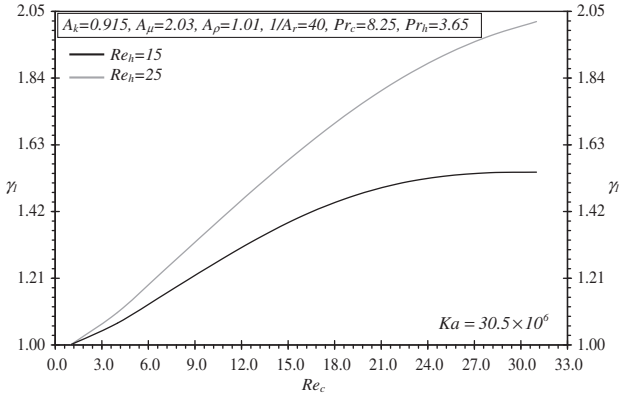

Fig. 5. Effects of Re_c on γ_1 for the flexible micro heat exchanger case.

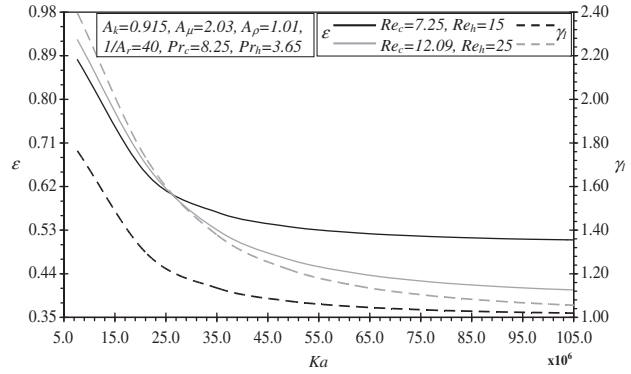

Fig. 6. Effects of Π_c on ε and γ_1 for the flexible micro heat exchanger case.

the separating plate increases. Thus, the maximum relative displacement A_d increases which augments the first performance indicator as shown in Fig. 7.

4.3. DL-flexible microchannel device

Fig. 8 shows that the second performance indicator (γ_2) is smaller than one for the small cold flow Reynolds numbers. This is expected because large pressure drops which induce large Reynolds numbers produce large moments of forces that can cause closing of flows passages. This effect increases γ_2 significantly above one. On the other hand, it is noticed from Fig. 9 that the second performance indicator is smaller than one for large stiffness numbers. Similar effects can be concluded for the role of the aspect ratio on the second performance indicator as shown in Fig. 10. It is seen

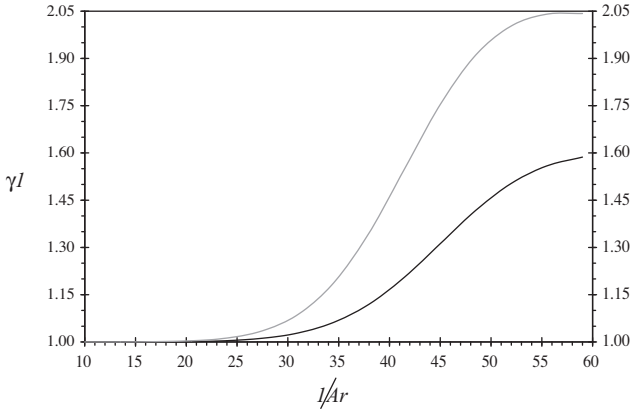

Fig. 7. Effects of $1/A_r$ on on γ_1 for the flexible micro heat exchanger case.

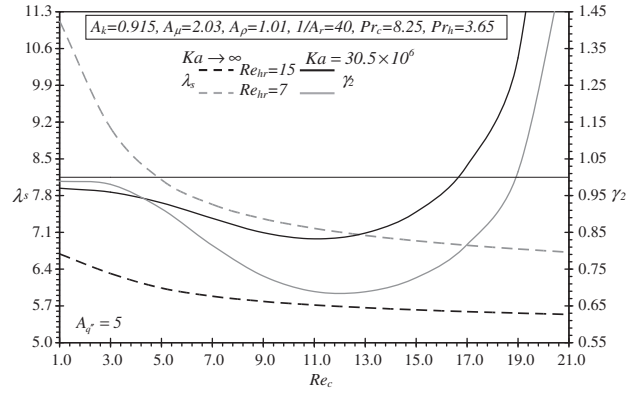

Fig. 8. Effects of Re_c on λ_s and γ_2 for the DL-flexible microchannel case.

from Figs. 8–10 that γ_2 has local minimum near the switch points. At these points, the increase in Re_c or the decrease in both Ka and A_r values cause the values of γ_2 to be larger than one. Therefore, the superiority of the heated microchannels with rotatable separating plates can be implied for moderate aspect ratios and moderate Reynolds and stiffness numbers. Typical heated plate temperature and Nusselt number distributions are shown in Fig. 11 for different cold flow Reynolds numbers.

4.4. Feasibility of the microchannels with rotatable separating plates devices

The inlet and outlet ports of the passages of the proposed device can be drilled on the upper and lower plates as shown in Fig. 1(a).

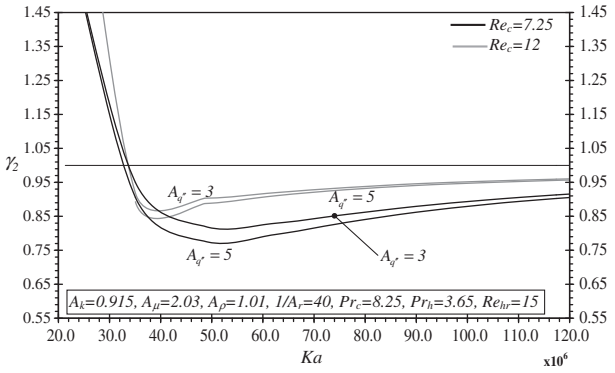

Fig. 9. Effects of Ka on γ_2 for the heated DL-flexible microchannel case.

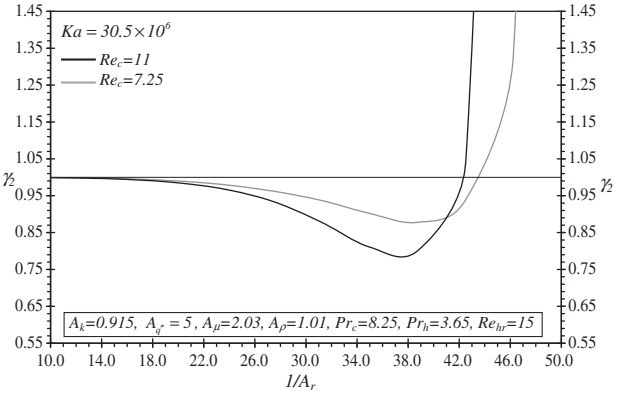

Fig. 10. Effects of Rec on λ_s and γ_2 for the DL-flexible microchannel case.

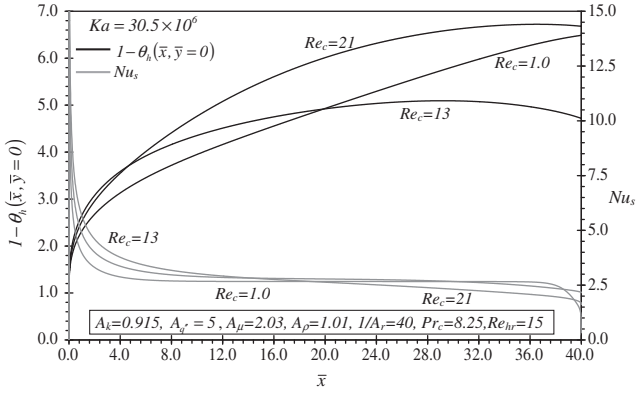

Fig. 11. Effects of Re_c and $\bar{x}$ on Nu_s and the surface temperature for the DL-flexible microchannel case.

For this configuration, changes in inlet and exit heights with operating conditions have no influence on inlet and exit port dimensions. Moreover, the expected leakage of fluid flow between the passages of the proposed device can be controlled by having well sealed separating plates using carefully designed soft seals. The manufacturing of these kinds of seals which should exhibit high softness, high strength and high anti-leaking sealant attributes is possible considering the current advanced fabrication methods. Finally, the possibility of having deflected separating plate other than that due to its rotation can be eliminated by having multiple micro-passages system within each layer [9]. For this case, each micro-passage is isolated against the other one by using sides made of anti-leaking soft seals which provide an additional support to the separating plate.

5. Conclusions

Heat transfer inside DL-microchannels devices with rotatable separating plates was considered in this work. Two different devices having different boundary conditions are analyzed. These are (A) the flexible micro heat exchanger and (B) the heated DL-flexible microchannels device. The rotational angle of the separating plate is related to the moment of pressure forces acting on it through the flexible supports. Appropriate forms of the coupled energy equations for both flows were solved using an iterative implicit-finite-difference method. The numerical results for case (A) were validated against obtained closed-form solutions based on fully developed thermal conditions.

It was found out that flexible micro heat exchangers always have a higher effectiveness than the rigid ones. Moreover, flexible micro heat exchangers were found to transfer more heat than the rigid ones operating under the same pumping power. Further, the DL-flexible microchannels device (device B) was found to provide more cooling effects per unit pumping power than the rigid devices for flow Reynolds numbers below specific values. In addition, the cooling attributes for device B were found to be better than those for the heated DL-rigid microchannels device at stiffness numbers and aspect ratios above certain values. These specific values were found to vary with the heat load. DL-microchannels devices with rotatable separating plates can be used in several applications such as electronic cooling.

References

[1] J.-Y. Jung, H.-S. Oh, H.-Y. Kwak, Forced convective heat transfer of nanofluids in microchannels, Int. J. Heat Mass Transfer 52 (2009) 466–472.
[2] D.B. Tuckerman, D.B. Pease, High-performance heat sinking for VLSI, IEEE Electron. Dev. Lett. EDL-2 (1981) 126–129.
[3] L.J. Missaggia, J.N. Walpole, Z.L. Liau, R.J. Philips, Microchannel heat sinks for two dimensional high-power-density diode laser arrays, IEEE J. Quant. Electron. 25 (1989) 1988–1992.
[4] M.B. Kleiner, S.A. Kuhn, K. Haberger, High performance forced air cooling scheme employing micro-channel heat exchangers 1, IEEE Trans. Compon. Pack. Manuf. Technol. Part A 18 (1995) 795–804.
[5] V.K. Samalam, Convective heat transfer in micro-channels, J. Electron. Mater. 18 (1989) 611–617.
[6] G.L. Morini, Single phase convection heat transfer in microchannels: a review of experimental results, Int. J. Thermal Sci. 43 (2004) 631–651.
[7] P.S. Lee, S.V. Garimella, D. Liu, Investigation of heat transfer in rectangular microchannels, Int. J. Heat Mass Transfer 48 (2005) 1688–1704.
[8] H.-C. Chiu, J.-H. Jang, H.-W. Yeh, M.-S. Wu, The heat transfer characteristics of liquid cooling heat sink containing micrchannels, Int. J. Heat Mass Transfer 54 (2011) 34–42.
[9] D.Y. Lee, K. Vafai, Comparative analysis of jet impingement and microchannel cooling for high heat flux applications, Int. J. Heat Mass Transfer 42 (1999) 1555–1568.
[10] A.G. Fedorov, R. Viskanta, Three-dimensional conjugate heat transfer in the microchannel heat sing for electronic packaging, Int. J. Heat Mass Transfer 43 (2000) 399–415.
[11] K. Vafai, L. Zhu, Analysis of a two-layered micro channel heat sink concept in electronic cooling, Int. J. Heat Mass Transfer 42 (1999) 2287–2297.
[12] T.M. Harms, M.J. Kazmierczak, F.M. Gerner, Developing convective heat transfer in deep rectangular microchannels, Int. J. Heat Fluid Flow 20 (1999) 149–157.
[13] Y. Sui, C.J. Teo, P.S. Lee, Y.T. Chew, C. Shu, Fluid flow and heat transfer in wavy microchannels, Int. J. Heat Mass Transfer 53 (2010) 2760–2772.
[14] A.D. Stroock, S. K.W. Dertinger, A. Ajdari, A. Ajdari, I. Mezic, G.M. Whitesides, Chaotic mixer for microchannels, Science 25 (2002) 647–651.
[15] A.-R.A. Khaled, K. Vafai, Cooling enhancements in thin films supported by flexible complex seals in the presence of ultrafine suspensions, J. Heat Transfer – Trans. ASME 125 (2003) 916–925.
[16] A.-R.A. Khaled, K. Vafai, Control of exit flow and thermal conditions using two-layered thin films supported by flexible complex seals, Int. J. Heat Mass Transfer 47 (2004) 1599–1611.
[17] A.-R.A. Khaled, K. Vafai, Analysis of thermally expandable flexible fluidic thin-film channels, J. Heat Transfer – Trans. ASME 129 (2007) 813–818.
[18] K. Vafai, A.-R.A. Khaled, Analysis of flexible microchannel heat sinks, Int. J. Heat Mass Transfer 48 (2005) 1739–1746.
[19] R.L. Norton, Machine Design: An Integrated Approach, second ed., Prentice-Hall, New Jersey, 1998.
[20] A.-R.A. Khaled, Analysis of heat transfer inside flexible thin- film channels with nonuniform height distributions, J. Heat Transfer – Trans. ASME 129 (2007) 401–404.
[21] C. Hong, Y. Asako, Heat transfer characteristics of gaseous flows in a microchannel and a microtube with constant wall temperature, Numer. Heat Transfer, Part A: Appl. 52 (2009) 219–238.
[22] S. Kaka, H. Liu, Heat Exchangers: Selection, Rating, and Thermal Design, CRC Press, Florida, 2001.
[23] F.P. Incorpera, D.P. DeWitt, T.L. Bergman, A.S. Lavine, Fundamentals of Heat and Mass Transfer, sixth ed., John Wiley, New York, 2006.
[24] F.G. Blottner, Finite-difference methods of solution of the boundary-layer equations, AIAA J. 8 (1970) 193–205.
[25] K. Vafai, J. Ettefagh, The effects of sharp corners on Buoyancy-driven flows with particular emphasis on outer boundaries, Int. J. Heat Mass Transfer 33 (1990) 2311–2328.